JGP Journal of General Physiology

ARTICLE

Voltage-Gated Na Channels

Differential state-dependent Nav1.8 inhibition by suzetrigine, LTGO-33, and A-887826

Sooyeon Jo[1*], Akie Fujita[1*], Tomás Osorno[1*], Robert G. Stewart[1*], Patric M. Vaelli[1], and Bruce P. Bean[1]

Nav1.8 sodium channels are expressed in pain-sensing neurons, and some Nav1.8 inhibitors significantly reduce pain in clinical trials. Several Nav1.8 inhibitors have an unusual state dependence whereby inhibition is relieved by depolarization. We compared the state-dependent action of several Nav1.8 channel inhibitors to test whether inhibition is relieved during action potential (AP) firing under physiological conditions to produce "reverse use dependence." A-887826 inhibition was substantially relieved by AP waveforms applied at 20 Hz at 37°C. In contrast, there was no relief during AP trains with suzetrigine (VX-548) or LTGO-33, even though inhibition could be effectively removed by long, strong depolarizations. These differences were explained by differences in the voltage dependence and kinetics with which the compounds dissociate from depolarized channels and rebind to resting state channels. Suzetrigine required the strongest depolarizations for relief (midpoint +33 mV) and relief was slow (tau >300 ms at +20 mV), so almost no relief occurred during an AP waveform. Relief from A-887826 required weaker depolarizations (midpoint +13 mV) and was much faster, so some relief occurred during each AP waveform and accumulated during 20-Hz trains. LTGO-33 required the weakest depolarizations for relief (midpoint −11 mV) and relief was even faster than for A-887826, but reinhibition between AP waveforms was far faster than for A-887826, so that relief did not accumulate during AP trains at 20 Hz. The results show that, unlike A-887826, there is no use-dependent relief of inhibition by suzetrigine or LTGO-33 with physiological voltage waveforms at physiological temperatures, but each for different reasons.

Introduction

Many drugs that inhibit voltage-dependent sodium channels interact with channels in a state-dependent manner. Most commonly, compounds bind more tightly to channels in the open or inactivated state than in the resting state. This state dependence is seen with local anesthetics like lidocaine (Hille, 1977) and anti-epileptic drugs like phenytoin, carbamazepine, lamotrigine, and lacosamide (Catterall, 1999; Sheets et al., 2008; Jo and Bean, 2017). Because recovery of channel availability is typically slowed after channels have bound the inhibitor during a depolarization (Hille, 1977), inhibition can build up during repeated depolarizations, the phenomenon of "use dependence," typical of many local anesthetics, antiarrhythmics, and antiseizure drugs (Hille, 1977; Catterall, 1999; Rogawski and Löscher, 2004).

Small-diameter dorsal root ganglion (DRG) neurons are unusual in that they possess a component of voltage-dependent sodium current that is resistant to tetrodotoxin (TTX), with distinct voltage dependence and slower activation and inactivation kinetics compared with TTX-sensitive sodium current (Kostyuk et al, 1981; Ogata and Tatebayashi, 1992; Roy and Narahashi, 1992; Elliott and Elliott, 1993; Cummins and Waxman, 1997; Rush et al, 1998, 2006; reviewed by Rush et al. [2007]). The major component of TTX-resistant sodium current is carried by Nav1.8 channels (Akopian et al., 1996; Sangameswaran et al., 1996; Renganathan et al., 2001; reviewed by Han et al. [2016]; Bennett et al. [2019]; Goodwin and McMahon [2021]). Because Nav1.8 channels are expressed in C-fiber pain-sensing neurons (nociceptors) and only a few other types of neurons (Han et al., 2016; Bennett et al., 2019; Zheng et al., 2019; Goodwin and McMahon, 2021), they have emerged as a potential target for new drugs to treat pain (reviewed by Alsaloum et al. [2020], [2025]). Recently, two new Nav1.8 inhibitors, VX-150 and VX-548 (now called suzetrigine), showed efficacy and safety in human clinical trials for reducing

[1]Department of Neurobiology, Harvard Medical School, Boston, MA, USA.

*S. Jo, A. Fujita, T. Osorno, and R.G. Stewart contributed equally to this paper. Correspondence to Bruce P. Bean: bruce_bean@hms.harvard.edu

This work is part of a special issue on Voltage-Gated Sodium (Na_v) Channels.

acute pain, stimulating interest in further development of Nav1.8 inhibitors (Hijma et al., 2021; Jones et al., 2023; Osteen et al., 2025).

Both VX-150 and VX-548 interact with Nav1.8 channels with an unusual state dependence, whereby the compounds show dramatic relief of inhibition by depolarization, suggesting greatly reduced affinity for binding to channels with voltage sensors in a depolarized position (Vaelli et al., 2024; Osteen et al., 2025). Similar relief of inhibition by depolarization is seen with other Nav1.8 inhibitors, including A-803467 (Browne et al., 2009a, 2009b; Jo et al., 2023), A-887826 (Jo et al., 2023), and LTGO-33 (Gilchrist et al., 2024). This state dependence can produce "reverse use dependence" with cumulative relief of inhibition by repeated depolarizations (Browne et al., 2009a, 2009b; Jo et al., 2023; Gilchrist et al., 2024; Vaelli et al., 2024). The relief of Nav1.8 inhibition by depolarization seen with these compounds reflects particular distinctive properties of the compounds rather than a general property of Nav1.8 channels because inhibition of Nav1.8 channels by lidocaine (Leffler et al., 2007), carbamazepine (Cardenas et al., 2006), cannabidiol (Zhang and Bean, 2021), and other small-molecule inhibitors (Leffler et al., 2010) is enhanced when channels are depolarized, producing conventional use dependence.

Reverse use dependence could be an undesirable feature of a sodium channel inhibitor if it occurred with repetitive firing of action potentials at physiological frequencies. In fact, a previous study found that A-887826 inhibition of Nav1.8 channels in mouse nociceptors could be dramatically relieved by action potential waveforms at 5 Hz (Jo et al., 2023). However, the voltage dependence and kinetics with which inhibition is relieved vary considerably among the different Nav1.8 inhibitors that have been studied, so it is difficult to predict how dramatic the effect would be with action potential waveforms. It is important to test for this at the physiological temperature since it is very likely that the kinetics of compound binding and unbinding to the different states of the channel are temperature-dependent. There are limitations to studying this in mouse neurons because there are major differences in the potency of the compounds for inhibiting mouse versus human Nav1.8 channels. For example, A-887826 is roughly 10 times more potent for inhibiting human Nav1.8 channels than mouse Nav1.8 channels (Jo et al., 2023), and VX-548 and LTGO-33 are even more selective for human over mouse Nav1.8 channels (Jones et al., 2023; Gilchrist et al., 2024; Osteen et al., 2025). In addition, the voltage dependence and gating of human and rat Nav1.8 channels are somewhat different (Han et al., 2015; Zhang et al., 2017), which is important when characterizing state dependence of drug action.

We explored the degree to which inhibition by A-887826, VX-548, and LTGO-33 can be relieved by repetitive action potentials, studying inhibition of cloned human Nav1.8 channels using action potential waveforms recorded from human sensory neurons and doing experiments at physiological temperature. We find prominent relief of inhibition by A-887826 but no relief of VX-548 or LTGO-33 inhibition by action potential waveforms. The differences can be explained by major differences in the kinetics with which inhibition is relieved during depolarizations and reestablished after depolarizations.

Materials and methods

Human Nav1.8 cell line

A cell line stably expressing human Nav1.8 α- and β3-subunits in Chinese hamster ovary (CHO-K1, RRID:CVCL_0214) cells was purchased from B'SYS GmbH and grown in Ham's F-12 medium (Corning) containing 10% FBS, 1% penicillin/streptomycin (Sigma-Aldrich), 3.5 µg/ml puromycin (Sigma-Aldrich), and 350 µg/ml hygromycin (Sigma-Aldrich) under 5% CO_2 at 37°C.

Electrophysiology

For electrophysiological recordings, cells were replated on coverslips for 1–6 h before recording. Whole-cell recordings were obtained using patch pipettes with resistances of 1.5–2.2 MΩ when filled with an internal solution consisting of 61 mM CsF, 61 mM CsCl, 9 mM NaCl, 1.8 mM $MgCl_2$, 1.8 mM EGTA, 14 mM creatine phosphate (tris salt), 4 mM MgATP, 0.3 mM GTP (tris salt), and 9 mM HEPES, pH adjusted to 7.2 with CsOH. The shank of the electrode was wrapped with parafilm to reduce capacitance and allow optimal series resistance compensation without oscillation. Seals were obtained and the whole-cell configuration was established with cells in Tyrode's solution consisting of 155 mM NaCl, 3.5 mM KCl, 1.5 mM $CaCl_2$, 1 mM $MgCl_2$, 10 mM HEPES, and 10 mM glucose, with pH adjusted to 7.4 with NaOH. After establishing whole-cell recording, cells were lifted off the bottom of the recording chamber and placed in front of an array of quartz flow pipes (250 µm internal diameter, 350 µm external, Polymicro Technologies) attached with styrene butadiene glue (Amazing Goop, Eclectic Products) to an aluminum rod (1 × 1 cm) whose temperature was controlled by resistive heating elements and a feedback-controlled temperature controller (TC-344B; Warner Instruments). Recordings were made using a base external solution of Tyrode's solution containing 200 nM TTX to inhibit a small endogenous TTX-sensitive sodium current (Vaelli et al., 2024) and 1 mg/ml Pluronic PF-68 (Sigma-Aldrich), a surfactant polaxamer without which the apparent potency of VX-548 was found to be reduced (Vaelli et al., 2024). Control external solutions contained the same concentration of DMSO as the matched drug-containing solutions. Solution changes were made (in <1 s) by moving the cell between adjacent pipes. All experiments were done at 37°C.

Compounds were applied long enough to reach steady-state inhibition and then the various voltage protocols were run. Steady-state inhibition was reached in about 3 min with 100 nM A-887826, 1 min with 1 nM VX-548, and 1 min with 300 nM LTGO-33.

Currents were recorded with either an Axon Instruments Multiclamp 700B amplifier (Molecular Devices) controlled by pClamp9.2 (RRID:SCR_011323) software (Axon Instruments), filtered at 5 kHz with a low-pass Bessel filter, and digitized at 50 kHz by a Digidata 1322A data acquisition interface, or recorded by a Sutter Instruments dPatch integrated amplifier/data acquisition system, with filtering at 10 kHz and digitization at 100 kHz. Amplifiers were tuned for partial compensation of series resistance (typically 70–80% of total series resistance of 4–10 MΩ), and tuning was periodically readjusted during the experiments. Data were analyzed using programs written in Igor Pro 6, 8, or 9 (Wavemetrics) using DataAccess (Bruxton Software) to read pClamp files into Igor Pro (RRID:SCR_000325).

The action potential waveform used for action potential clamp experiments was recorded from a neuron dissociated from the DRG of an adult human donor using a preparation generously prepared by the AnaBios Corporation. This neuron was capsaicin-sensitive (41 nA current evoked by 10 μM capsaicin). The action potential was evoked by a brief (0.5 ms) injection of a large current (6.5 nA) so that the action potential waveform was not influenced by the current injection. The action potential waveform was chosen for having typical characteristics of action potentials recorded in other capsaicin-sensitive human DRG neurons at 37°C, with a resting potential of −75 mV, a threshold near −44 mV, a peak at +44 mV, and with a broad shoulder typical of C-fiber nociceptors, with a width at half-maximum amplitude of 2.53 ms. The action potential was recorded with an internal solution of 139.5 mM K-gluconate, 13.5 mM NaCl, 1.62 mM $MgCl_2$, 9 mM HEPES, 0.99 mM EGTA, 0.09 mM $CaCl_2$, 14 mM creatine phosphate (tris salt), 4 mM MgATP, and 0.3 mM GTP (tris salt), pH adjusted to 7.2 with KOH and an external Tyrode's solution of 155 mM NaCl, 3.5 mM KCl, 1.5 mM $CaCl_2$, 1 mM $MgCl_2$, 10 mM HEPES, and 10 mM glucose, pH adjusted to 7.4 with NaOH. In applying the voltage waveform as a command in experiments with the Nav1.8 cell line that used a CsF/CsCl-based internal solution, 8 mV was subtracted from the waveform to account for a liquid junction potential of −13 mV between the K-gluconate-based pipette solution and the bath Tyrode's solution in which the pipette current was zeroed before making a seal in the recording of the action potential and a junction potential of −5 mV between the CsF/CsCl-based internal solution of the pipette solution and the bath Tyrode's solution when the pipette was zeroed in the voltage clamp experiments.

For both step depolarizations and the action potential waveform, currents were corrected for linear capacitative and leak currents, which were determined using 5 mV hyperpolarizations delivered from the resting potential and then appropriately scaled and subtracted.

To quantify the voltage dependence with which inhibition was relieved by 100-ms depolarizing pulses in the protocol shown in Fig. 2, current during the test pulse (after a 10-ms return to −80 mV to allow recovery from fast inactivation) was plotted as a function of the voltage of the prepulse and fit with a Boltzmann function $\{I_{min} + (I_{max} - I_{min})*[1/(1 + \exp(-(V_m - V_h)/k))]\}$ to data from minimum to maximum, where I_{min} is the minimum current, I_{max} is the maximum current, V_m is the voltage of the prepulse, V_h is the midpoint, and k is the slope factor.

All experiments were exploratory, and statistical results of mean ± standard error of the mean (SEM) are descriptive and are presented to enable evaluation of reproducibility rather than for hypothesis testing (Michel et al., 2020).

Compounds

A-887826 (Zhang et al., 2010) was obtained from Sigma-Aldrich, prepared as a stock solution of 10 mM in DMSO, and stored as frozen aliquots at −20°C.

The active enantiomer of VX-548 was synthesized as described in Vaelli et al. (2024), prepared as a 1 mM stock solution in DMSO (Sigma-Aldrich), further diluted to 1 or 10 μM in DMSO, and stored as frozen aliquots at −20°C. We verified that this synthesis resulted in a compound with identical potency and properties as the VX-548 compound ("suzetrigine") now available commercially (MedChemExpress).

The active isomer of LTGO-33 was synthesized at BioDuro-Sundia following the procedure published in the patent literature (WO 2022/192487; PCT/US2022/019673).

Control external solutions contained the same concentration of DMSO as the matched drug-containing solutions. All external solutions included 1 mg/ml Pluronic PF-68, and drug-containing solutions were sonicated for 2 min while heated to 30°C.

Results

Tests for relief of inhibition by action potential waveforms

To explore how state-dependent inhibition is affected by repetitive action potential waveforms under physiological conditions, we did voltage clamp experiments at the physiological temperature (37°C), recording sodium currents from cloned human Nav1.8 channels in a stable cell line using as a voltage command an action potential waveform previously recorded in a human DRG neuron at 37°C. This neuron was capsaicin-sensitive (as determined by the application of 10 μM capsaicin in voltage clamp) and had action potentials with the broad shoulder typical of C-fiber nociceptors. In voltage clamp, the action potential waveform evoked Nav1.8 current with two distinct phases (Fig. 1, A, C, and E): a fast phase of current during the rising phase of the action potential followed by a dip (corresponding to the reduced driving force for sodium current at the peak of the action potential) and then a plateau of current during the shoulder of the action potential. The pattern of activation of Nav1.8 current during both the rising phase and shoulder of the action potential is very similar to previous action potential clamp recordings of TTX-resistant sodium current during the action potential of capsaicin-sensitive rat DRG neurons studied at 22°C (Blair and Bean, 2002), suggesting that Nav1.8 channels contribute to both the fast rising phase and the broad shoulder of the action potential of human nociceptors at physiological temperature, as they do in rat neurons at room temperature.

To explore the characteristics of Nav1.8 inhibitors under conditions mimicking nociceptor firing, we applied the action potential waveform at a frequency of 20 Hz, near the upper limit for firing frequencies of C-fiber nociceptors in a high state of activity. In control, there was a reduction by about 15% of the action potential–evoked current over a train of 98 action potentials delivered at 20 Hz. Because the time at −75 mV between action potential waveforms is long (~46 ms) compared with the time-course of recovery from fast inactivation of human Nav1.8 channels at 37°C, which we found had a time constant of 0.8 ms, the reduction in current during the train of action potentials likely corresponds to a process of slow inactivation previously described for TTX-resistant sodium current in rat and mouse DRG neurons (Ogata and Tatebayashi, 1992; Rush et al., 1998; Choi et al., 2007; Zhang and Bean, 2021). Interestingly, the degree of cumulative slow activation of human Nav1.8 channels by about 15% during action potentials applied at 20 Hz at 37°C is less

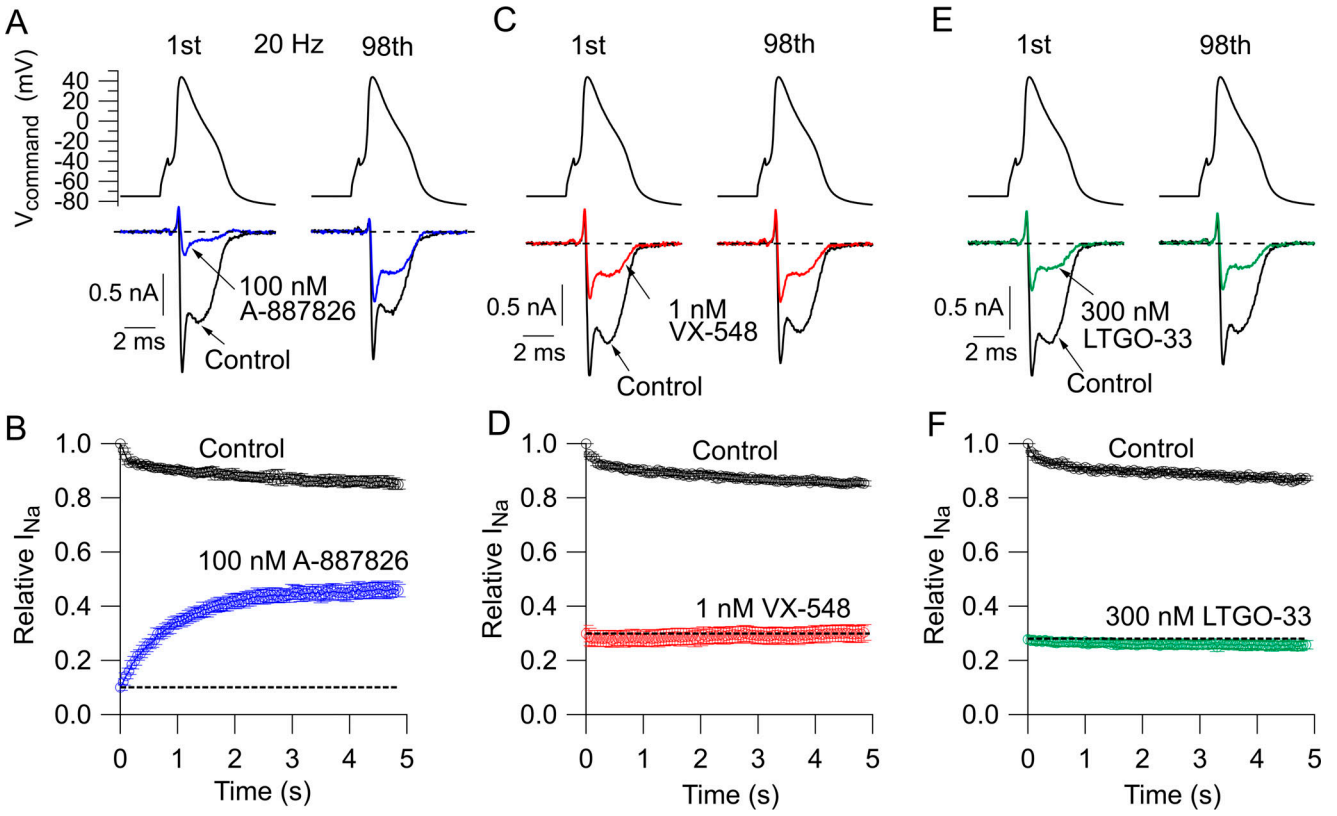

Figure 1. **Test for reverse use dependence using an AP waveform recorded from a human DRG neuron at 37°C, delivered at 20 Hz. (A)** Currents evoked by the 1st and 98th AP waveform delivered at 20 Hz, before and after application of 100 nM A-887826. **(B)** Collected results showing current normalized to the maximal current in control (mean ± SEM, n = 7). **(C and D)** Same for application of 1 nM VX-548 (n = 10). **(E and F)** Same for application of 300 nM LTGO-33 (n = 7).

than a reduction of ~20% seen with TTX-resistant sodium current in rat DRG neurons with action potentials delivered at a much lower frequency (1 Hz) at 22°C (Blair and Bean, 2003), suggesting that human Nav1.8 channels might have less prominent slow inactivation than rat Nav1.8 channels.

We first studied inhibition by A-887826, a Nav1.8 inhibitor (Zhang et al., 2010), previously found to have the property of depolarization-induced relief (Jo et al., 2023; Vaelli et al., 2024). Inhibition by A-887826 showed prominent relief of inhibition during AP trains (Fig. 1, A and B). With 100 nM A-887826, AP-evoked current during the train increased from 0.10 ± 0.01 (normalized to initial resting control) at the beginning to 0.46 ± 0.02 at the end of the train (mean ± SEM, n = 7).

In contrast, there was negligible reverse use dependence during the AP trains by VX-548 (Fig. 1, C and D), another Nav1.8 inhibitor that shows strong relief of inhibition by long, strong depolarizations (Vaelli et al., 2024). We selected a concentration of 1 nM VX-548 to study because it produced reasonably strong inhibition (to about 30% of control) while leaving enough current so that any changes could be well-resolved. 1 nM VX-548 inhibited current evoked by the first action potential to 0.30 ± 0.03 of control, and the current evoked by the 98th AP was exactly the same (0.30 ± 0.03, mean ± SEM, n = 10). Similarly, inhibition of AP-evoked current by LTGO-33 (Fig. 1, E and F), another Nav1.8 inhibitor showing effective relief by long, strong depolarizations (Gilchrist et al., 2024), was not relieved during the AP train (reduction to 0.28 ± 0.02 in the first action potential and to 0.26 ± 0.02 in the 98th action potential; mean ± SEM, n = 7).

Voltage dependence of relief of inhibition

We next sought to understand these differences by examining the voltage dependence and kinetics with which inhibition is relieved by depolarization and restored during repolarization. Fig. 2 shows an experiment testing the voltage dependence of relief of inhibition by A-887826, VX-548, and LTGO-33. A 100-ms prepulse to varying voltages up to +120 mV is followed by a 10-ms return to −80 mV to allow recovery of channels from fast inactivation and then by a test pulse to +10 mV to assay channel availability. In control, channel availability decreases by ~30% as the 100-ms prepulse increases, reflecting channels entering slow inactivation during the prepulse. In striking contrast to the progressive reduction of test pulse current by depolarizing prepulses in control, in the presence of each of the three inhibitors, the test pulse current increases with more depolarized prepulses. A simple interpretation of this effect is that the drug unbinds during more positive prepulses and that the 10-ms return to −80 mV is too short to allow complete rebinding of the drug. The results show that the voltage dependence of relief of inhibition is quite different for the different compounds, occurring with a midpoint of +13 ± 1 mV for A-887826, +33 ± 4 mV for VX-548, and −11 ± 4 mV for LTGO-33 (mean ± SEM, n = 7 for

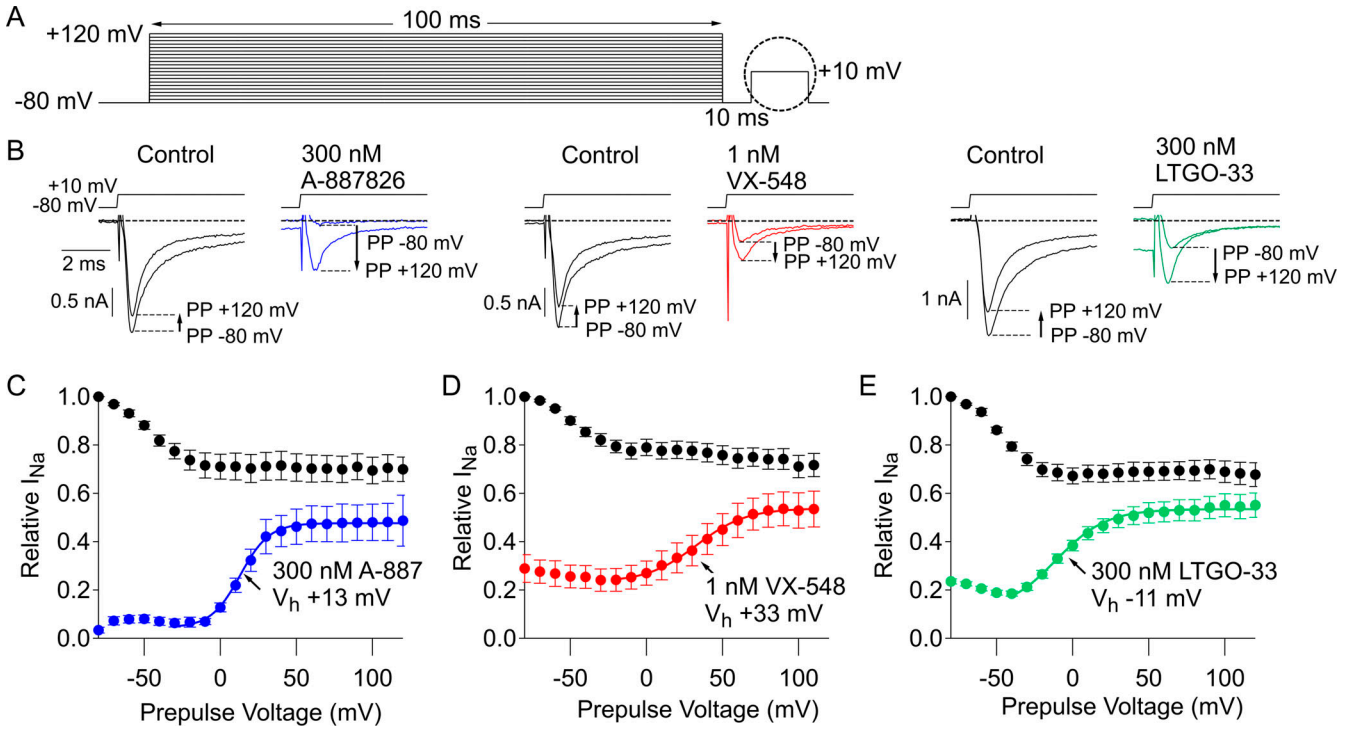

Figure 2. **Voltage dependence of relief of inhibition by A-887826, VX-548, and LTGO-33. (A)** Voltage protocol for assaying relief of inhibition. A 100-ms prepulse to varying voltages is followed by a test pulse to +10 mV to assay channel availability after returning to −80 mV for 10 ms to allow channels to recover from fast inactivation. **(B)** Examples of test pulse currents evoked after the prepulses to −80 and +120 mV in control (left) and after application of each inhibitor (right). **(C)** Test pulse currents versus prepulse voltage in control (black) and with 300 nM A-887826 (blue, mean ± SEM, *n* = 7). Solid line: Boltzmann function with midpoint +13 mV and slope factor 9.6 mV (mean values for individual fits to data from the seven cells). **(D)** Same for 1 nM VX-548 (red, *n* = 7). Solid line: Boltzmann function with midpoint +33 mV, slope factor 16.3 mV. **(E)** Same for 300 nM LTGO-33 (green, *n* = 7). Solid line: Boltzmann function with midpoint −11 mV, slope factor 16.5 mV.

all). Interestingly, at least for VX-548, the voltage dependence of relief of inhibition occurs at much more negative voltages at 37°C than near-room temperature (midpoint of +57 mV at 27°C, Vaelli et al., 2024), underscoring the importance of making measurements at physiological temperature to evaluate reverse use dependence.

Kinetics of relief of inhibition

Fig. 3 shows the results of an experiment measuring the kinetics with which inhibition is relieved at various voltages. Fig. 3 A illustrates the experimental protocol, assaying relief of A-887826 inhibition at +100 mV. A series of depolarizations are given to +100 mV with increasing duration, starting with a short (0.3 ms) step. After each step, the membrane potential is returned to −80 mV for 10 ms to allow recovery from fast inactivation, and a test step to +10 mV then assays the fraction of sodium channels that are drug-free and able to open. This protocol was applied to test the time-course of relief of inhibition at various voltages from 0 to +100 mV. Plotting the current in each test pulse as a function of the total cumulative time at the voltage of interest showed that the time course of relief of inhibition by each compound was strongly dependent on the voltage but with different kinetics for the three compounds. Fig. 3 B shows the time course of relief at +20, +40, and +100 mV for A-887826. At each voltage, the time course of relief could be fit well by a single exponential. Relief of inhibition became faster with stronger depolarizations, with the time constant for relief from A-887826 inhibition decreasing from 64 ms at +20 mV to 5.9 ms at +100 mV. Fig. 3 C shows the results of the same experimental protocol with 300 nM LTGO-33 and Fig. 3 D with 1 nM VX-548.

Fig. 3 E shows the collected results of this experiment for the three different inhibitors. The kinetics of relief for A-887826 and LTGO-33 were similar, with slightly faster relief from LTGO-33 at each voltage. The time course of relief from VX-548 inhibition was far slower. For example, the time constant for relief at +40 mV was 127 ± 85 ms for VX-548, 22 ± 9 ms for A-887826, and 16 ± 6 ms for LTGO-33 (mean ± SEM, *n* = 5, 7, and 17).

Kinetics of reinhibition

We next tested the kinetics with which inhibition is reestablished when channels return to the resting state at −80 mV after being relieved by depolarization. Fig. 4 A shows the voltage protocol. Maximal relief was produced by a 200-ms depolarization to +100 mV, and the time course of reinhibition was assayed by short (0.3 ms) test pulses to +10 mV delivered at various times after the end of the depolarization, ranging from 3 ms to 50 s. The time course of reinhibition could be fit well by a single exponential, with very different kinetics for the three different compounds. Reinhibition by A-887826 was very slow, with a time constant of 6.4 s with 300 nM A-887826. Reinhibition by VX-548 was faster, with a time constant of 2.0 s with 1 nM VX-548. Reinhibition by LTGO was far faster than for the

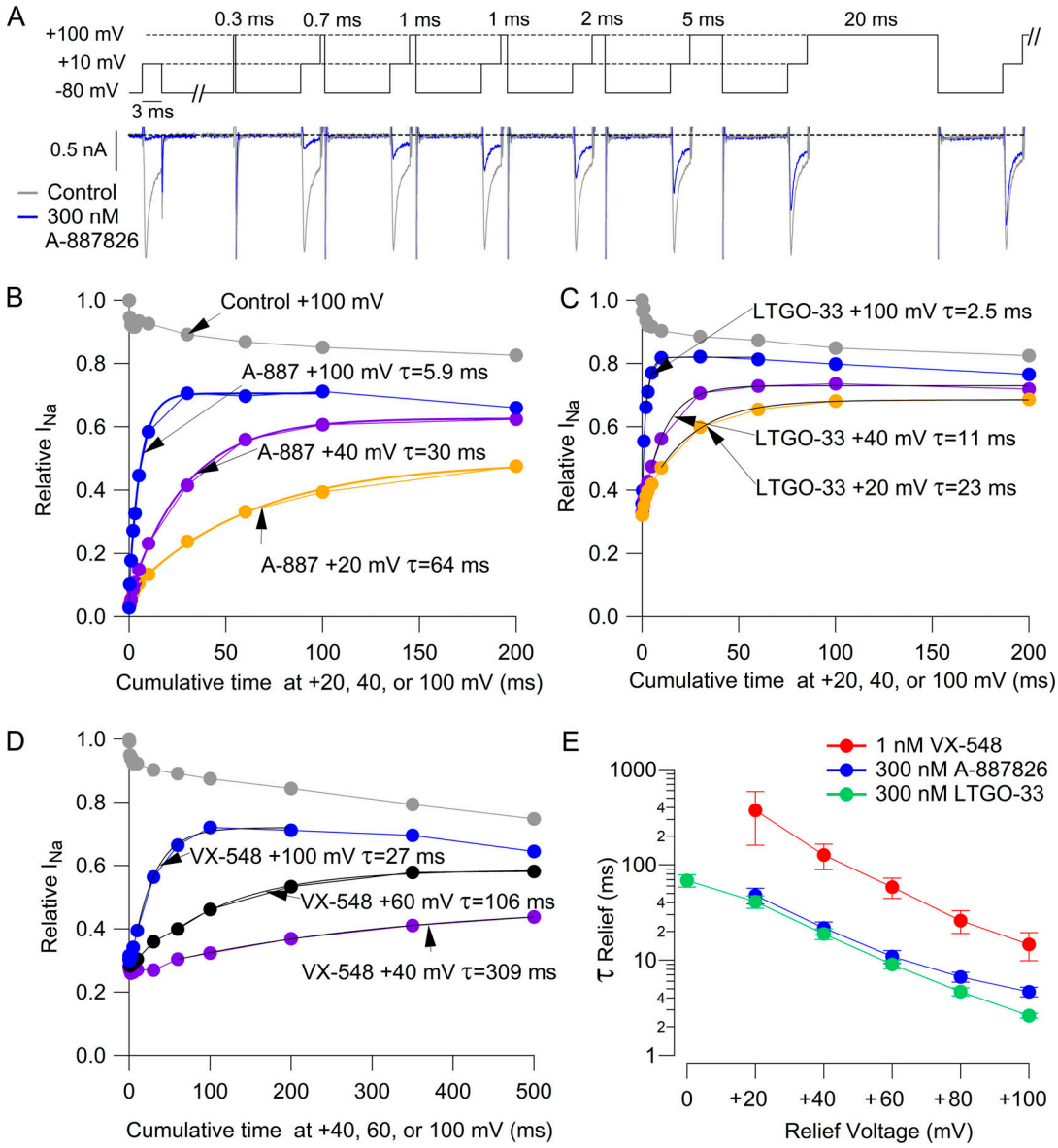

Figure 3. **Time-course of relief of inhibition by A-887826, VX-548, and LTGO-33 at different voltages. (A)** Time-course of relief of inhibition by 300 nM A-887826 at +100 mV determined with a single-sweep protocol. Fraction of drug-free channels was assayed by short (3 ms) test steps to +10 mV, each following a 10-ms period at −80 mV to allow recovery from fast inactivation. A succession of depolarizations to +100 mV of various durations produced progressive relief of inhibition by A-887826 (blue trace). The protocol continued with increasing durations of the steps. **(B)** Channel availability during the test steps to +10 mV as a function of cumulative time when this protocol was applied with depolarizations to +20, +40, and +100 mV (data from a single cell). Data points are fitted with single exponential functions with the indicated time constants. **(C)** Same for an experiment with 300 nM LTGO-33. **(D)** Same for an experiment with 1 nM VX-548. **(E)** Collected data for time constant of relief as a function of voltage for VX-548, A-887826, and LTGO-33, respectively. Mean ± SEM, *n* = 5, 7, and 17 for VX-548, A-887826, and LTGO-33.

other two inhibitors, with a time constant of 71 ms with 300 nM LTGO-33.

Discussion

The vast majority of small-molecule sodium channel inhibitors used clinically as local anesthetics, anti-epileptics, and antiarrhythmics have a form of state-dependent inhibition whereby the drugs bind more tightly to depolarized states of the channel (Hille, 1977; Catterall, 1999). This state dependence has two consequences that probably underlie the ability of the drugs to produce beneficial clinical effects without excessive disruption of normal excitability. First, inhibition is enhanced by small, steady depolarizations as a consequence of tighter binding to inactivated channels because in most neurons and muscles, the fraction of channels in the higher-affinity inactivated state increases dramatically with steady depolarization of the resting potential by only 5–10 mV. In central neurons, epileptic activity often produces steady depolarization associated with an increase in external potassium so that enhancement of inhibition can preferentially disrupt the excitability of epileptic foci with less effect on other neurons. In cardiac muscle, ventricular

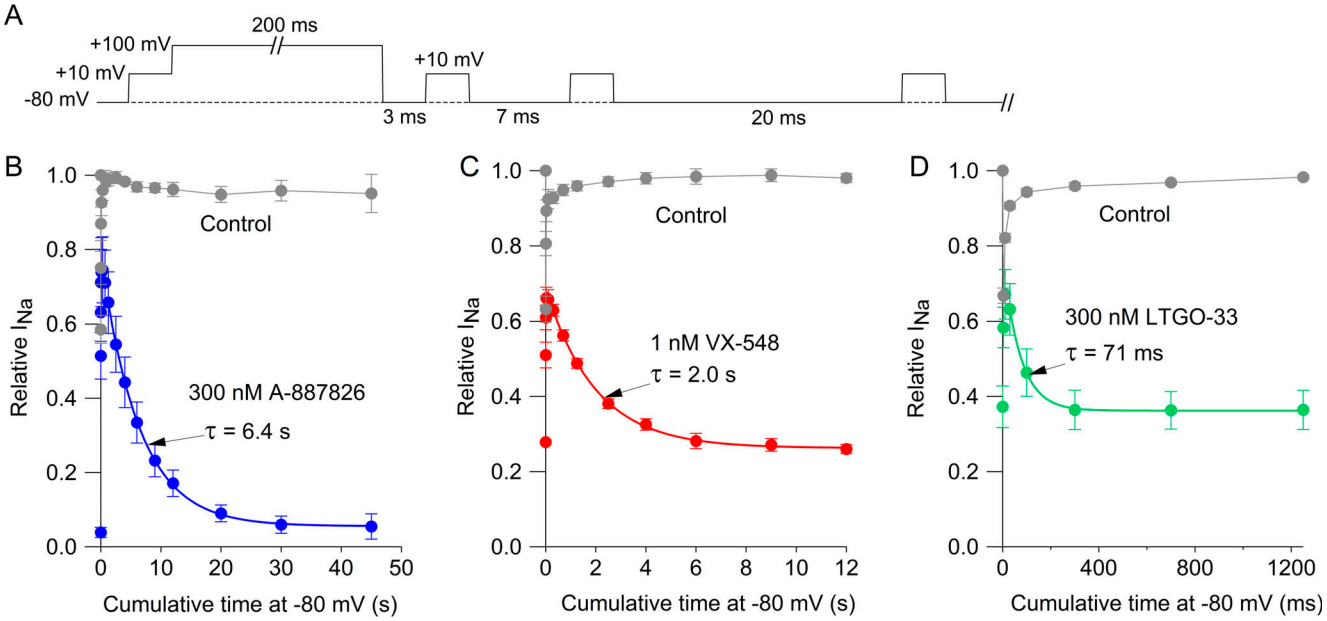

Figure 4. **Time-course of reinhibition following relief of inhibition. (A)** Voltage protocol for examining the time course of reinhibition. Relief of inhibition is produced by a 200-ms step to +100 mV and channel availability is assayed by a series of test pulses to +10 mV delivered at various times after the long prepulse. The test pulses are short (3 ms) to minimize entry into slow inactivation or relief of inhibition during the test pulse. **(B)** Time-course of reinhibition in 300 nM A-887826. Peak current during each test pulse is normalized to maximal current availability in control, determined by the test pulse to +10 mV preceding the 200-ms prepulse in control. Data points show mean ± SEM (n = 7) and are fitted with a single exponential function (smooth line). **(C)** Same for 1 nM VX-548 (n = 7). **(D)** Same for 300 nM LTGO-33 (n = 10).

arrhythmias often result from ischemic areas, where the resting potential is depolarized so that sodium channels are partially inactivated and conduction is slowed so that action potentials arrive at a healthier tissue after the refractory period, producing re-entrant arrhythmias; preferential inhibition by antiarrhythmics of sodium channels in these depolarized areas can block such re-entrant pathways. A second consequence of tight binding to depolarized states of the channel is the phenomenon of use dependence, whereby more rapid firing of action potentials—for example in epileptic foci or nociceptors with strong painful stimuli—produces a frequency-dependent inhibition as a consequence of accumulation of channels in drug-bound open or inactivated states.

Based on these considerations, opposite state dependence in which inhibition is relieved by depolarization would seem undesirable. However, our results show that although A-887826, VX-548, and LTGO-33 share this unusual state dependence only A-887826 shows substantial reverse use dependence with physiological action potentials at physiological temperatures. Interestingly, the lack of reverse use dependence by VX-548 and LTGO-33 compared with A-887826 occurs for two different reasons. In the case of VX-548, relief of inhibition requires much larger depolarizations (midpoint +33 mV) compared with A-887826 (midpoint +13 mV), and in addition, the kinetics of relief are much slower for VX-548 compared with A-887826. Although the action potential of human nociceptors reaches a peak near +45 mV, where there is substantial relief by VX-548 in the steady state, the kinetics of relief (tau of 127 ms at +40 mV) are so slow that there is evidently negligible unbinding of drug during the action potential, which repolarizes to 0 mV—a voltage where there is almost no steady-state relief of VX548 inhibition—within 1.6 ms. With A-887826, relief is much faster (tau of 22 ms at +40 and 48 ms at +20 mV) so that there is some loss of drug with each action potential. Although the loss of drug with each action potential is very small, the loss accumulates steadily during a 5-s train of action potentials at 20 Hz because the ~46-ms period at resting voltages between action potentials is not long enough to allow substantial rebinding of the drug, which occurs with a time constant of 6.4 s.

Our results show that the reason that LTGO-33 does not show reverse use dependence with physiological action potential frequencies is completely different than for VX-548. LTGO-33 inhibition is relieved more effectively by depolarization than that of A-887826 (midpoint of −11 mV for LTGO-33 versus +13 mV for A-887826), and relief is also faster (time constants of 16 ms at +40 mV and 35 ms at +20 mV for LTGO-33 versus 22 ms at +40 mV and 48 ms at +20 mV for A-887826). Clearly, LTGO-33 unbinds from channels during an action potential more effectively than A-887826. What prevents significant use-dependent relief of LTGO-33 inhibition during trains of action potentials is that rebinding at the resting voltage in between action potentials is much faster (tau of 71 ms with 300 nM LTGO-33) compared with A-887826 (tau of 6.4 s with 300 nM A-887826). Thus, with each cycle, some LTGO-33 inhibition is relieved during the action potential waveform, but is restored by rebinding in between the action potentials.

For all three inhibitors, substantial relief of inhibition requires far larger steady depolarizations than would be achieved by steady depolarization of the resting potential by 5–10 mV, even though such depolarizations can put a substantial fraction

of channels into the inactivated state. Thus, it is clear that not all inactivated channels have a low affinity for the drugs. Mutagenesis experiments suggest that LTGO-33 acts at a site formed by an extracellular cleft formed by S1, S3, and S4 helices along with the S3–S4 linker region of the voltage sensor region of domain II (Gilchrist et al., 2024) and that VX-548 binds at a similar site (Osteen et al., 2025). Presumably, the conformation of the binding pocket changes when the voltage sensor moves from the "down" to the "up" position upon depolarization. With this picture, relief of inhibition is not produced by channels entering the inactivated state, as for binding of local anesthetics, but by movement of the voltage sensor of domain II, which occurs over a more depolarized voltage range associated with activation rather than steady-state inactivation. Moreover, if a compound binds more tightly to the resting state of the voltage sensor than to the depolarized state, it will stabilize the resting state relative to the depolarized state so that movement of the voltage sensor will be shifted to more depolarized voltages with the compound bound. Thus, the voltage dependence of relief of inhibition will be shifted in the depolarized direction compared with the normal voltage dependence of movement of the sensor in the absence of the drug, with the degree of shift greater with a greater difference in drug affinity for the resting versus depolarized state. The considerable difference in the voltage dependence of relief between LTGO-33 (midpoint –11 mV) and VX-548 (midpoint +33 mV) can then be interpreted as differences in binding affinity to the resting versus depolarized state of the voltage sensor of the different compounds. VX-548 would have the largest difference in affinity for resting versus depolarized positions of the voltage sensor and LTGO-33 the lowest. It remains to be determined whether A-887826 interacts with the channels in the same general binding site.

More than the differences in voltage dependence of relief, the results suggest that it is the kinetics of relief and kinetics of reinhibition that are crucial for determining whether or not a compound will show substantial reverse use dependence with physiological firing patterns. A-887826 shows reverse use dependence largely because reinhibition is extremely slow such that even a small amount of relief with each action potential builds up during a train. LTGO-33 shows minimal reverse use dependence because reinhibition is so much faster than with A-887826. It is not clear what structural elements of the different compounds produce such large differences in reinhibition kinetics, especially because the potencies of A-887826 and LTGO-33 are comparable.

In testing for reverse use dependence, we performed experiments at 37°C with the expectation that both the action potential waveform and the kinetics of drug binding and unbinding are likely to be temperature-dependent. A somewhat unexpected observation was that the voltage dependence with which VX-548 inhibition is relieved by depolarization is quite different at 37°C (midpoint +33 mV) than at 27°C (midpoint +57 mV, Vaelli et al., 2024). The less depolarized voltage dependence of relief suggests that reverse use dependence could be more evident at physiological temperature than room temperature. However, for both VX-548 and LTGO-33, our results show that even at 37°C, there is no relief with physiological action potential waveforms, as was seen in similar experiments at room temperature (Gilchrist et al., 2024; Osteen et al., 2025).

In testing for reverse use dependence, we selected concentrations of inhibitors that produced inhibition to about 10–30% of control before delivering the use-dependent protocols. This level of current remaining allowed good resolution when testing for reverse use dependence. Consideration of the concentration dependence of drug action (Vaelli et al., 2024) suggests that the extent of reverse use dependence is likely to be reduced as concentrations of the drug increase. For VX-548, A-887826, and VX-150m (closely related structurally to LTGO-33), the kinetics of relief of inhibition during depolarization had no dependence on drug concentration, while reinhibition when membrane potential was repolarized increased roughly linearly with drug concentration. During trains of depolarizing steps or action potential waveforms, drug unbinding during the depolarization would occur to the same extent in different drug concentrations but rebinding would be faster in higher concentrations, resulting in less reverse use dependence.

In conditions of inflammation, there can be an increase in action potential height and width (Dang et al., 2008; Qiu et al., 2021; Tiwari et al., 2023), likely related to an increase in the size of Nav1.8 current (Tanaka et al., 1998; Black et al., 2004; Beyak et al., 2004; Tan et al., 2014; Qiu et al., 2021). A wider action potential would be expected to produce more dramatic reverse use dependence with A-887826, but it seems unlikely that the relatively modest changes in action potential peak and width would result in substantial reverse use dependence with VX-548 or LTGO-33. For A-887826 or other Nav1.8 inhibitors with substantial reverse use dependence, enhanced reverse use dependence could combine with upregulated Nav1.8 current to reduce efficacy in inhibiting nociceptor excitability under conditions of inflammation.

Overall, the results show that depolarization-induced relief of inhibition is unlikely to be a limitation in the therapeutic use of VX-548 or potential therapeutic use of LTGO-33 but suggest that in developing new Nav1.8 inhibitors, it will be useful to test not only for the presence of depolarization-induced relief of inhibition but also to characterize the kinetics of relief and reinhibition, ideally at the physiological temperature. The fact that the overall effect of the drugs depends on the kinetics of state-dependent drug unbinding and rebinding also serves as a reminder of the limits of even the best static cryo-EM structures and models of binding sites to capture important features of drug action.

Data availability

All the data supporting the findings of this study are embodied in the figures. Excel files of the data are available upon reasonable request to the corresponding author.

Acknowledgments

Jeanne M. Nerbonne served as editor.

We are very grateful to the anonymous donor and family for providing the human DRG neuron used to record the action potential waveform and to Richard Kondo, Kevin Carlin, Alyssa

Ferraiuolo, Gabrielle Bautista, and Christina Mai of the AnaBios Corporation for processing and arranging transfer of the preparation of the human DRG tissue. We are grateful to Dr. Jinbo Lee and Dr. Xiao Ma for advice on synthesis of VX-548 and LTGO-33.

This work was supported by National Institutes of Health grant R35-NS127216.

Author contributions: S. Jo: Conceptualization, Investigation, Methodology, Validation, Visualization, Writing - review & editing, A. Fujita: Conceptualization, Investigation, Methodology, Validation, Visualization, Writing - review & editing, T. Osorno: Conceptualization, Investigation, Methodology, Validation, Visualization, Writing - review & editing, R.G. Stewart: Conceptualization, Data curation, Formal analysis, Investigation, Methodology, Writing - original draft, Writing - review & editing, P.M. Vaelli: Conceptualization, Methodology, B.P. Bean: Conceptualization, Formal analysis, Funding acquisition, Methodology, Project administration, Supervision, Visualization, Writing - original draft, Writing - review & editing.

Disclosures: The authors declare no competing interests exist.

Submitted: 29 October 2024
Revised: 18 February 2025
Accepted: 9 March 2025

References

Akopian, A.N., L. Sivilotti, and J.N. Wood. 1996. A tetrodotoxin-resistant voltage-gated sodium channel expressed by sensory neurons. *Nature*. 379:257–262. https://doi.org/10.1038/379257a0

Alsaloum, M., S.D. Dib-Hajj, D.A. Page, P.C. Ruben, A.R. Krainer, and S.G. Waxman. 2025. Voltage-gated sodium channels in excitable cells as drug targets. *Nat. Rev. Drug Discov.* https://doi.org/10.1038/s41573-024-01108-x

Alsaloum, M., G.P. Higerd, P.R. Effraim, and S.G. Waxman. 2020. Status of peripheral sodium channel blockers for non-addictive pain treatment. *Nat. Rev. Neurol.* 16:689–705. https://doi.org/10.1038/s41582-020-00415-2

Bennett, D.L., A.J. Clark, J. Huang, S.G. Waxman, and S.D. Dib-Hajj. 2019. The role of voltage-gated sodium channels in pain signaling. *Physiol. Rev.* 99:1079–1151. https://doi.org/10.1152/physrev.00052.2017

Beyak, M.J., N. Ramji, K.M. Krol, M.D. Kawaja, and S.J. Vanner. 2004. Two TTX-resistant Na+ currents in mouse colonic dorsal root ganglia neurons and their role in colitis-induced hyperexcitability. *Am. J. Physiol. Gastrointest. Liver Physiol.* 287:G845–G855. https://doi.org/10.1152/ajpgi.00154.2004

Black, J.A., S. Liu, M. Tanaka, T.R. Cummins, and S.G. Waxman. 2004. Changes in the expression of tetrodotoxin-sensitive sodium channels within dorsal root ganglia neurons in inflammatory pain. *Pain*. 108:237–247. https://doi.org/10.1016/j.pain.2003.12.035

Blair, N.T., and B.P. Bean. 2002. Roles of tetrodotoxin (TTX)-sensitive Na+ current, TTX-resistant Na+ current, and Ca2+ current in the action potentials of nociceptive sensory neurons. *J. Neurosci.* 22:10277–10290. https://doi.org/10.1523/JNEUROSCI.22-23-10277.2002

Blair, N.T., and B.P. Bean. 2003. Role of tetrodotoxin-resistant Na+ current slow inactivation in adaptation of action potential firing in small-diameter dorsal root ganglion neurons. *J. Neurosci.* 23:10338–10350. https://doi.org/10.1523/JNEUROSCI.23-32-10338.2003

Browne, L.E., F.E. Blaney, S.P. Yusaf, J.J. Clare, and D. Wray. 2009a. Structural determinants of drugs acting on the Nav1.8 channel. *J. Biol. Chem.* 284:10523–10536. https://doi.org/10.1074/jbc.M807569200

Browne, L.E., J.J. Clare, and D. Wray. 2009b. Functional and pharmacological properties of human and rat NaV1.8 channels. *Neuropharmacology*. 56:905–914. https://doi.org/10.1016/j.neuropharm.2009.01.018

Cardenas, C.A., C.G. Cardenas, A.J. de Armendi, and R.S. Scroggs. 2006. Carbamazepine interacts with a slow inactivation state of NaV1.8-like sodium channels. *Neurosci. Lett.* 408:129–134. https://doi.org/10.1016/j.neulet.2006.08.070

Catterall, W.A. 1999. Molecular properties of brain sodium channels: An important target for anticonvulsant drugs. *Adv. Neurol.* 79:441–456.

Choi, J.-S., S.D. Dib-Hajj, and S.G. Waxman. 2007. Differential slow inactivation and use-dependent inhibition of Nav1.8 channels contribute to distinct firing properties in IB4+ and IB4- DRG neurons. *J. Neurophysiol.* 97:1258–1265. https://doi.org/10.1152/jn.01033.2006

Cummins, T.R., and S.G. Waxman. 1997. Downregulation of tetrodotoxin-resistant sodium currents and upregulation of a rapidly repriming tetrodotoxin-sensitive sodium current in small spinal sensory neurons after nerve injury. *J. Neurosci.* 17:3503–3514. https://doi.org/10.1523/JNEUROSCI.17-10-03503.1997

Dang, K., K. Lamb, M. Cohen, K. Bielefeldt, and G.F. Gebhart. 2008. Cyclophosphamide-induced bladder inflammation sensitizes and enhances P2X receptor function in rat bladder sensory neurons. *J. Neurophysiol.* 99:49–59. https://doi.org/10.1152/jn.00211.2007

Elliott, A.A., and J.R. Elliott. 1993. Characterization of TTX-sensitive and TTX-resistant sodium currents in small cells from adult rat dorsal root ganglia. *J. Physiol.* 463:39–56. https://doi.org/10.1113/jphysiol.1993.sp019583

Gilchrist, J.M., N.-D. Yang, V. Jiang, and B.D. Moyer. 2024. Pharmacologic characterization of LTGO-33, a selective small molecule inhibitor of the voltage-gated sodium channel $Na_V1.8$ with a unique mechanism of action. *Mol. Pharmacol.* 105:233–249. https://doi.org/10.1124/molpharm.123.000789

Goodwin, G., and S.B. McMahon. 2021. The physiological function of different voltage-gated sodium channels in pain. *Nat. Rev. Neurosci.* 22:263–274. https://doi.org/10.1038/s41583-021-00444-w

Han, C., M. Estacion, J. Huang, D. Vasylyev, P. Zhao, S.D. Dib-Hajj, and S.G. Waxman. 2015. Human Na(v)1.8: Enhanced persistent and ramp currents contribute to distinct firing properties of human DRG neurons. *J. Neurophysiol.* 113:3172–3185. https://doi.org/10.1152/jn.00113.2015

Han, C., J. Huang, and S.G. Waxman. 2016. Sodium channel Nav1.8: Emerging links to human disease. *Neurology*. 86:473–483. https://doi.org/10.1212/WNL.0000000000002333

Hijma, H.J., P.S. Siebenga, M.L. de Kam, and G.J. Groeneveld. 2021. A phase 1, randomized, double-blind, placebo-controlled, crossover study to evaluate the pharmacodynamic effects of VX-150, a highly selective NaV1.8 inhibitor, in healthy male adults. *Pain Med.* 22:1814–1826. https://doi.org/10.1093/pm/pnab032

Hille, B. 1977. Local anesthetics: Hydrophilic and hydrophobic pathways for the drug-receptor reaction. *J. Gen. Physiol.* 69:497–515. https://doi.org/10.1085/jgp.69.4.497

Jo, S., and B.P. Bean. 2017. Lacosamide inhibition of Nav1.7 voltage-gated sodium channels: Slow binding to fast-inactivated states. *Mol. Pharmacol.* 91:277–286. https://doi.org/10.1124/mol.116.106401

Jo, S., H.B. Zhang, and B.P. Bean. 2023. Use-dependent relief of inhibition of Nav1.8 channels by A-887826. *Mol. Pharmacol.* 103:221–229. https://doi.org/10.1124/molpharm.122.000593

Jones, J., D.J. Correll, S.M. Lechner, I. Jazic, X. Miao, D. Shaw, C. Simard, J.D. Osteen, B. Hare, A. Beaton, et al. 2023. Selective inhibition of $Na_V1.8$ with VX-548 for acute pain. *N. Engl. J. Med.* 389:393–405. https://doi.org/10.1056/NEJMoa2209870

Kostyuk, P.G., N.S. Veselovsky, and A.Y. Tsyndrenko. 1981. Ionic currents in the somatic membrane of rat dorsal root ganglion neurons-I. Sodium currents. *Neuroscience*. 6:2423–2430. https://doi.org/10.1016/0306-4522(81)90088-9

Leffler, A., J. Reckzeh, and C. Nau. 2010. Block of sensory neuronal Na+ channels by the secreolytic ambroxol is associated with an interaction with local anesthetic binding sites. *Eur. J. Pharmacol.* 630:19–28. https://doi.org/10.1016/j.ejphar.2009.12.027

Leffler, A., A. Reiprich, D.P. Mohapatra, and C. Nau. 2007. Use-dependent block by lidocaine but not amitriptyline is more pronounced in tetrodotoxin (TTX)-Resistant Nav1.8 than in TTX-sensitive Na+ channels. *J. Pharmacol. Exp. Ther.* 320:354–364. https://doi.org/10.1124/jpet.106.109025

Michel, M.C., T.J. Murphy, and H.J. Motulsky. 2020. New author guidelines for displaying data and reporting data analysis and statistical methods in experimental biology. *Mol. Pharmacol.* 97:49–60. https://doi.org/10.1124/mol.119.118927

Ogata, N., and H. Tatebayashi. 1992. Slow inactivation of tetrodotoxin-insensitive Na+ channels in neurons of rat dorsal root ganglia. *J. Membr. Biol.* 129:71–80. https://doi.org/10.1007/BF00232056

Osteen, J.D., S. Immani, T.L. Tapley, T. Indersmitten, N.W. Hurst, T. Healey, K. Aertgeerts, P.A. Negulescu, and S.M. Lechner. 2025. Pharmacology

and mechanism of action of suzetrigine, a potent and selective $Na_V1.8$ pain signal inhibitor for the treatment of moderate to severe pain. *Pain Ther.* https://doi.org/10.1007/s40122-024-00697-0

Qiu, J., X. Xu, S. Zhang, G. Li, and G. Zhang. 2021. Modulations of $Na_v1.8$ and $Na_v1.9$ channels in monosodium urate-induced gouty arthritis in mice. *Inflammation*. 44:1405–1415. https://doi.org/10.1007/s10753-021-01425-y

Renganathan, M., T.R. Cummins, and S.G. Waxman. 2001. Contribution of Na(v)1.8 sodium channels to action potential electrogenesis in DRG neurons. *J. Neurophysiol.* 86:629–640. https://doi.org/10.1152/jn.2001.86.2.629

Rogawski, M.A., and W. Löscher. 2004. The neurobiology of antiepileptic drugs. *Nat. Rev. Neurosci.* 5:553–564. https://doi.org/10.1038/nrn1430

Roy, M.L., and T. Narahashi. 1992. Differential properties of tetrodotoxin-sensitive and tetrodotoxin-resistant sodium channels in rat dorsal root ganglion neurons. *J. Neurosci.* 12:2104–2111. https://doi.org/10.1523/JNEUROSCI.12-06-02104.1992

Rush, A.M., M.E. Bräu, A.A. Elliott, and J.R. Elliott. 1998. Electrophysiological properties of sodium current subtypes in small cells from adult rat dorsal root ganglia. *J. Physiol.* 511:771–789. https://doi.org/10.1111/j.1469-7793.1998.771bg.x

Rush, A.M., T.R. Cummins, and S.G. Waxman. 2007. Multiple sodium channels and their roles in electrogenesis within dorsal root ganglion neurons. *J. Physiol.* 579:1–14. https://doi.org/10.1113/jphysiol.2006.121483

Rush, A.M., S.D. Dib-Hajj, S. Liu, T.R. Cummins, J.A. Black, and S.G. Waxman. 2006. A single sodium channel mutation produces hyper- or hypoexcitability in different types of neurons. *Proc. Natl. Acad. Sci. USA*. 103:8245–8250. https://doi.org/10.1073/pnas.0602813103

Sangameswaran, L., S.G. Delgado, L.M. Fish, B.D. Koch, L.B. Jakeman, G.R. Stewart, P. Sze, J.C. Hunter, R.M. Eglen, and R.C. Herman. 1996. Structure and function of a novel voltage-gated, tetrodotoxin-resistant sodium channel specific to sensory neurons. *J. Biol. Chem.* 271:5953–5956. https://doi.org/10.1074/jbc.271.11.5953

Sheets, P.L., C. Heers, T. Stoehr, and T.R. Cummins. 2008. Differential block of sensory neuronal voltage-gated sodium channels by lacosamide [(2R)-2-(acetylamino)-N-benzyl-3-methoxypropanamide], lidocaine, and carbamazepine. *J. Pharmacol. Exp. Ther.* 326:89–99. https://doi.org/10.1124/jpet.107.133413

Tan, Z.-Y., A.D. Piekarz, B.T. Priest, K.L. Knopp, J.L. Krajewski, J.S. McDermott, E.S. Nisenbaum, and T.R. Cummins. 2014. Tetrodotoxin-resistant sodium channels in sensory neurons generate slow resurgent currents that are enhanced by inflammatory mediators. *J. Neurosci.* 34:7190–7197. https://doi.org/10.1523/JNEUROSCI.5011-13.2014

Tanaka, M., T.R. Cummins, K. Ishikawa, S.D. Dib-Hajj, J.A. Black, and S.G. Waxman. 1998. SNS Na+ channel expression increases in dorsal root ganglion neurons in the carrageenan inflammatory pain model. *Neuroreport*. 9:967–972. https://doi.org/10.1097/00001756-199804200-00003

Tiwari, M.N., B.E. Hall, A.-T. Ton, R. Ghetti, A. Terse, N. Amin, M.-K. Chung, and A.B. Kulkarni. 2023. Activation of cyclin-dependent kinase 5 broadens action potentials in human sensory neurons. *Mol. Pain*. 19:17448069231218353. https://doi.org/10.1177/17448069231218353

Vaelli, P., A. Fujita, S. Jo, H.-X.B. Zhang, T. Osorno, X. Ma, and B.P. Bean. 2024. State-dependent inhibition of Nav1.8 channels by VX-150 and VX-548. *Mol. Pharmacol.* 106:298–308. https://doi.org/10.1124/molpharm.124.000944

Zhang, H.B., and B.P. Bean. 2021. Cannabidiol inhibition of murine primary nociceptors: Tight binding to slow inactivated states of Nav1.8 channels. *J. Neurosci.* 41:6371–6387. https://doi.org/10.1523/JNEUROSCI.3216-20.2021

Zhang, X., B.T. Priest, I. Belfer, and M.S. Gold. 2017. Voltage-gated Na^+ currents in human dorsal root ganglion neurons. *Elife*. 6.e23235. https://doi.org/10.7554/eLife.23235

Zhang, X.-F., C.-C. Shieh, M.L. Chapman, M.A. Matulenko, A.H. Hakeem, R.N. Atkinson, M.E. Kort, B.E. Marron, S. Joshi, P. Honore, et al. 2010. A-887826 is a structurally novel, potent and voltage-dependent Na(v)1.8 sodium channel blocker that attenuates neuropathic tactile allodynia in rats. *Neuropharmacology*. 59:201–207. https://doi.org/10.1016/j.neuropharm.2010.05.009

Zheng, Y., P. Liu, L. Bai, J.S. Trimmer, B.P. Bean, and D.D. Ginty. 2019. Deep sequencing of somatosensory neurons reveals molecular determinants of intrinsic physiological properties. *Neuron*. 103:598–616.e7. https://doi.org/10.1016/j.neuron.2019.05.039